

LNF-94/037(P)

**$\gamma\gamma \rightarrow \pi^0 \pi^0$ and $\eta \rightarrow \pi^0 \gamma\gamma$ at Low Energy Within the
Extended Nambu Jona-Lasinio Model***

S. Bellucci, C. Bruno

Nuclear Physics B 452, 626-645, (1995)



$\gamma\gamma \rightarrow \pi^0\pi^0$ and $\eta \rightarrow \pi^0\gamma\gamma$ at low energy within the extended Nambu Jona-Lasinio model^{*}

S. Bellucci¹, C. Bruno²

INFN-Laboratori Nazionali di Frascati, P.O. Box 13, I-00044 Frascati, Italy

Received 2 February 1995; revised 2 May 1995; accepted 14 July 1995

Abstract

Within the Extended Nambu Jona-Lasinio model, we calculate the $O(p^6)$ counterterms entering the low-energy expansion of the $\gamma\gamma \rightarrow \pi^0\pi^0$ and the $\eta \rightarrow \pi^0\gamma\gamma$ amplitudes in Chiral Perturbation Theory. For $\gamma\gamma \rightarrow \pi^0\pi^0$ our results are compatible with both the experimental data and the two-loop calculation using meson resonance saturation. For the η decay we find $\Gamma(\eta \rightarrow \pi^0\gamma\gamma) = 0.58 \pm 0.3$ eV which is in agreement with experiment within one standard deviation. We also give predictions for the neutral pion polarizabilities and compare them with the results obtained from resonance saturation.

1. Introduction

Over the last few years the transitions $\gamma\gamma \rightarrow \pi^0\pi^0$ and $\eta \rightarrow \pi^0\gamma\gamma$ have been studied in the framework of Chiral Perturbation Theory (χ PT). These two processes have in common the fact that their amplitude starts at $O(p^4)$ and that there is no contribution from tree diagrams at this lowest order.

The first transition has recently been analysed in [1] at the two-loop level. The $O(p^6)$ counterterms have been evaluated assuming resonance saturation and it is shown that the predicted cross-section fits well the existing data [2]. It has been noted by several authors [3–6] that the contribution of these counterterms to the cross-section is very small in the threshold region. On the other hand, when not only high-precision data

^{*} Work supported in part by the EEC Human Capital and Mobility Program.

¹ E-mail: bellucci@lnf.infn.it.

² Also at: Institute for Theoretical Physics, University of Bern, Sidlerstrasse 5, CH-3012 Bern, Switzerland; E-mail: cbruno@butp.unibe.ch.

from DAΦNE become available for energies up to 600 MeV, but also the theoretical predictions are improved by an unitarization procedure (this requires calculating the full $\gamma\gamma \rightarrow \pi^+\pi^-$ amplitude to two-loops), it may become possible to extract one linear combination of the $O(p^6)$ coupling constants.

Concerning $\eta \rightarrow \pi^0\gamma\gamma$ a particular feature of this decay is that the $O(p^4)$ one-loop contribution to the width is more than two orders of magnitude smaller than the experimental measurement. In [7] this suppression has been explained in physical terms and a partial analysis of higher-loop contributions has been carried out. It is expected that the contribution of the $O(p^6)$ counterterms should account for a large part of the amplitude. The analysis of [7] gives a reasonable estimate of the order of magnitude for the decay width. However the latter is still a factor two smaller than the experimental value [8] $\Gamma(\eta \rightarrow \pi^0\gamma\gamma) = 0.85 \pm 0.18$ eV. New data may become available in the foreseeable future at SATURNE in Saclay, where a proposal for measuring this decay width has been recently approved.

The S -matrix elements for both transitions depend on the same set of $O(p^6)$ coupling constants. Throughout the following we restrict ourselves to the large N_c -limit, where only three low-energy couplings enter these transitions. The theoretical analysis is not yet refined enough and the present experiments are not sufficiently precise, to extract the value of these coupling constants from the data. Therefore it is important to make predictions for these couplings (this is particularly relevant in the case of the $\eta \rightarrow \pi^0\gamma\gamma$ decay width which has a strong dependence on the counterterms). One possibility is to estimate their value using the resonance saturation method, which provides successful predictions to $O(p^4)$ [9,10]. However it is not known whether the $O(p^6)$ couplings are actually saturated by resonance exchange. In addition to the estimate based on resonance saturation, one can find in the literature a calculation of two of the $O(p^6)$ coupling constants using the chiral quark model [4].

The purpose of our paper is to compute the three $O(p^6)$ coupling constants of the large N_c -limit in the framework of the Extended Nambu Jona-Lasinio (ENJL) model. Within this model the low-energy effective action of QCD has been derived [11] to $O(p^4)$, as well as some of the coupling constants governing the low-energy behaviour of the lowest spin-1 and spin-0 resonances [11,12]. The model has only three parameters (which is an advantage compared to the resonance saturation method where the number of parameters increases when new transitions and higher chiral order are considered) and the agreement with experiment is good.

This paper is organized as follows. In Section 2 we present the structure of the $O(p^6)$ chiral Lagrangian in the large N_c -limit. Section 3 contains the expressions for the amplitudes of the transitions and the pion polarizabilities. Section 4 is devoted to the ENJL predictions for the $O(p^6)$ coupling constants. Finally in Section 5 we discuss the numerical results and compare our predictions with those of the resonance saturation method and with the existing data.

2. $O(p^6)$ chiral Lagrangian

Let us collect as usual the octet of Goldstone bosons in the unitary unimodular matrix U

$$U = \exp \left(-i\sqrt{2} \frac{\Phi_8(x) + \Phi_1(x)}{f_0} \right), \quad (1)$$

where $f_0 \simeq f_\pi = 93.2$ MeV and $(\vec{\lambda})$ are Gell-Mann's $SU(3)$ matrices with $\text{tr} \lambda_a \lambda_b = 2\delta_{ab}$)

$$\Phi_8(x) = \frac{\vec{\lambda}}{\sqrt{2}} \cdot \vec{\Phi}_8(x) = \begin{pmatrix} \frac{\pi^0}{\sqrt{2}} + \frac{\eta_8}{\sqrt{6}} & \pi^+ & K^+ \\ \pi^- & \frac{-\pi^0}{\sqrt{2}} + \frac{\eta_8}{\sqrt{6}} & K^0 \\ K^- & \bar{K}^0 & -2\frac{\eta_8}{\sqrt{6}} \end{pmatrix}, \quad (2)$$

$$\Phi_1(x) = \frac{1}{\sqrt{3}} \eta_1 I. \quad (3)$$

The axial-vector field matrix ξ_μ is defined as follows:

$$\xi_\mu = i\{\xi^\dagger[\partial_\mu - ir_\mu]\xi - \xi[\partial_\mu - il_\mu]\xi^\dagger\} = i\xi^\dagger D_\mu U \xi^\dagger, \quad (4)$$

where $\xi\xi^\dagger = U$ and l_μ, r_μ are external 3×3 left and right field matrices. We also define

$$f_{(\pm)}^{\mu\nu} = \xi F_L^{\mu\nu} \xi^\dagger \pm \xi^\dagger F_R^{\mu\nu} \xi, \quad (5)$$

where $F_{L,R}^{\mu\nu}$ are the external field-strength tensors

$$\begin{aligned} F_L^{\mu\nu} &= \partial^\mu l^\nu - \partial^\nu l^\mu - i[l^\mu, l^\nu], \\ F_R^{\mu\nu} &= \partial^\mu r^\nu - \partial^\nu r^\mu - i[r^\mu, r^\nu]. \end{aligned} \quad (6)$$

Since we are only concerned with $f_{(+)}$ we set in what follows $f_{(+)}^{\mu\nu} = f^{\mu\nu}$. The specification to the electromagnetic field reads

$$F_L^{\mu\nu} = F_R^{\mu\nu} = |e|QF^{\mu\nu}, \quad (7)$$

where $Q = \text{diag}(2/3, -1/3, -1/3)$ is the quark charge matrix. Finally we shall need

$$\chi^+ = \xi^\dagger \chi \xi^\dagger + \xi \chi^\dagger \xi, \quad (8)$$

with

$$\chi = 2B_0 \mathcal{M}, \quad (9)$$

where $\mathcal{M} = \text{diag}(m_u, m_d, m_s)$ and B_0 is related to the vacuum expectation value

$$\langle \bar{q}q \rangle = -f_0^2 B_0 (1 + O(\mathcal{M})). \quad (10)$$

The structure of the strong chiral Lagrangian up to $O(p^4)$ has been studied in [14]. It is straightforward to write the relevant $O(p^6)$ chiral Lagrangian involving two neutral

pseudoscalar mesons and two photons. By restricting ourselves to the operators whose coupling constants are leading in the large- N_c limit we can write

$$\mathcal{L}^{(6)} = \frac{2}{f_\pi^2} \{d_1 \text{tr}(\xi^\alpha \xi_\beta f_{\alpha\mu} f^{\beta\mu}) + d_2 \text{tr}(\xi_\mu \xi^\mu f_{\alpha\beta} f^{\alpha\beta}) + d_3 \text{tr}(\chi^+ f_{\alpha\beta} f^{\alpha\beta})\}. \quad (11)$$

We have considered here that all quantities were commuting since we are interested only in neutral particles. Our conventions and notation are chosen in such a way that the expansion of this Lagrangian in terms of pseudoscalar fields coincides with the analogous expansion of the Lagrangian (4.28) in [1] which was introduced for the $SU(2)_L \times SU(2)_R$ case.

In the following section we display how the physical amplitudes are expressed in terms of these three coupling constants d_1 , d_2 and d_3 .

3. Amplitudes in χ PT

The Lorentz covariant and gauge invariant amplitudes for

$$\begin{aligned} \gamma(q_1)\gamma(q_2) &\rightarrow \pi^0(p_1)\pi^0(p_2) \quad \text{and} \\ \eta(p_1) &\rightarrow \pi^0(p_2)\gamma(q_1)\gamma(q_2) \end{aligned}$$

read

$$A = e^2 \epsilon_\mu(q_1) \epsilon_\nu(q_2) V_{\mu\nu}, \quad (12)$$

where

$$\begin{aligned} V_{\mu\nu} &= A(s, t, u) T_{1\mu\nu} + B(s, t, u) T_{2\mu\nu}, \\ T_{1\mu\nu} &= \frac{s}{2} g_{\mu\nu} - q_{1\nu} q_{2\mu}, \\ T_{2\mu\nu} &= 2s \Delta_\mu \Delta_\nu - (t - u)^2 g_{\mu\nu} - 2(t - u)(q_{1\nu} \Delta_\mu - q_{2\mu} \Delta_\nu), \\ \Delta_\mu &= (p_1 - p_2)_\mu. \end{aligned} \quad (13)$$

3.1. $\gamma\gamma \rightarrow \pi^0\pi^0$

For the $\gamma\gamma \rightarrow \pi^0\pi^0$ amplitude the Lagrangian (11) generates the $O(p^6)$ counterterms

$$\begin{aligned} A_6^N &= \frac{20}{9f_\pi^4} [16(d_3^r - d_2^r)m_\pi^2 + (d_1^r + 8d_2^r)s] + \dots, \\ B_6^N &= -\frac{10}{9f_\pi^4} d_1^r + \dots. \end{aligned} \quad (14)$$

We refer to Ref. [1] for the calculation in $SU(2)_L \times SU(2)_R$ of the additional contributions coming from chiral loops indicated here by the ellipses. The contribution of one kaon loop in the $O(p^4)$ amplitude has been computed in [15]. For s far below the

$K\bar{K}$ threshold it is numerically small, with respect to the contribution of one pion loop, owing to an extra factor $s/48m_K^2$ [16,6]. The calculation of the two-loop amplitude in $SU(3)_L \times SU(3)_R$ has not been carried out.

As in [1] one connects the constants a_1^r , a_2^r and b^r parametrizing the renormalized amplitudes

$$\begin{aligned} A_6^N &= \frac{a_1^r m_\pi^2 + a_2^r s}{(16\pi^2 f_\pi^2)^2} + \dots, \\ B_6^N &= \frac{b^r}{(16\pi^2 f_\pi^2)^2} + \dots, \end{aligned} \quad (15)$$

with the constants d_i^r

$$\begin{aligned} \frac{a_1^r}{(16\pi^2 f_\pi^2)^2} &= \left(\frac{20}{9f_\pi^4}\right) 16(d_3^r - d_2^r), \\ \frac{a_2^r}{(16\pi^2 f_\pi^2)^2} &= \left(\frac{20}{9f_\pi^4}\right) (d_1^r + 8d_2^r), \\ \frac{b^r}{(16\pi^2 f_\pi^2)^2} &= -\left(\frac{10}{9f_\pi^4}\right) d_1^r. \end{aligned} \quad (16)$$

3.2. $\eta \rightarrow \pi^0 \gamma \gamma$

For the η decay we have [7]

$$\begin{aligned} A_6^\eta &= \frac{4\sqrt{2}}{3\sqrt{2} f_\pi^4} [16(d_3^r m_\pi^2 - d_2^r m_\eta^2) + (d_1^r + 8d_2^r)s] + \dots, \\ B_6^\eta &= -\frac{2\sqrt{2}}{3\sqrt{2} f_\pi^4} d_1^r + \dots. \end{aligned} \quad (17)$$

In these expressions we have included the contribution of d_3 which has not been taken into account in [7]. However the size of this contribution is small because $m_\pi^2 \ll m_\eta^2$. The mixing $\eta - \eta'$ has been treated within χ PT in [14,17]. As a result the physical η is a superposition

$$\eta = \cos \theta \eta_8 - \sin \theta \eta_1, \quad (18)$$

with $\sin \theta \simeq -\frac{1}{3}$.

For the expressions of the $O(p^4)$ one-loop contribution to this process we refer to Ref. [7]. As explained there, this contribution is very small because pion loops violate G-parity and kaon loops are suppressed by a factor $1/24m_K^2$. The two-loop calculation has never been performed but the same argument can be advocated [7], to claim that loop contributions to the $O(p^6)$ amplitude are suppressed. In addition, consistency of the χ PT expansion implies that they are smaller than the $O(p^4)$ one-loop contribution.

On the other hand at $O(p^8)$ a new type of one-loop contribution appears by taking two anomalous vertices of $O(p^4)$. As shown in [7] the latter has an order of magnitude

comparable with the $O(p^4)$ one-loop contribution. This fact does not break the perturbative χ PT expansion because the higher order corrections to this $O(p^8)$ one-loop term will be small with respect to it.

Because all these loop contributions are small with respect to the measured decay width, one should expect that the $O(p^6)$ counterterms account for a large part of the full amplitude.

3.3. Neutral pion polarizabilities

The polarizabilities characterize the electric and magnetic properties of a composite system. They appear as parameters in the low-energy expansion of the Compton amplitudes at threshold [18]

$$T^{\text{Compton}} = 2 \left[\boldsymbol{\epsilon}_1 \cdot \boldsymbol{\epsilon}_2^* \left(\frac{\alpha}{m_\pi} - \alpha^N \omega_1 \omega_2 \right) - \beta^N (\mathbf{q}_1 \times \boldsymbol{\epsilon}_1) \cdot (\mathbf{q}_2 \times \boldsymbol{\epsilon}_2^*) + \dots \right], \quad (19)$$

where $q_i^\mu = (\omega_i, \mathbf{q}_i)$. Following the Condon-Shortley phase convention we define

$$\begin{aligned} (\alpha + \beta)^N &= 8\alpha m_\pi \lim_{s \rightarrow 0} \lim_{t \rightarrow m_\pi^2} B, \\ (\alpha - \beta)^N &= \frac{\alpha}{m_\pi} \lim_{s \rightarrow 0} \lim_{t \rightarrow m_\pi^2} (A + 8m_\pi^2 B). \end{aligned} \quad (20)$$

The one-loop amplitude calculated in [15,16] has been used in Eqs. (20), in order to find the neutral pion polarizabilities to $O(p^4)$, as discussed in Refs. [19,20]. Taking into account the full $O(p^6)$ result one gets [1]

$$\begin{aligned} (\alpha - \beta)^N &= -\frac{\alpha}{48\pi^2 m_\pi f_\pi^2} - \alpha m_\pi \frac{80}{9f_\pi^4} (d_1^r + 4d_2^r - 4d_3^r) + (\alpha - \beta)_{2\text{-loop}}^N, \\ (\alpha + \beta)^N &= -\alpha m_\pi \frac{80}{9f_\pi^4} d_1^r + (\alpha + \beta)_{2\text{-loop}}^N, \end{aligned} \quad (21)$$

where the two-loop contributions can be obtained from Table 3 in [1]³

$$\begin{aligned} (\alpha - \beta)_{2\text{-loop}}^N &\simeq -0.31, \\ (\alpha + \beta)_{2\text{-loop}}^N &\simeq 0.17. \end{aligned} \quad (22)$$

The latter numerical values have been derived for the $SU(2)_L \times SU(2)_R$ case; we are neglecting the additional two-loop contributions for the $SU(3)_L \times SU(3)_R$ case due to kaon loops. Notice that the kaon-loop contribution to the one-loop amplitude, calculated in [15], vanishes for $s \rightarrow 0$. Hence, at the one-loop level, there is no kaon-loop contribution to the pion polarizabilities, according to (20).

³ The values of the polarizabilities are in units of 10^{-4} fm^3 in what follows.

4. ENJL model prediction for the coupling constants

The idea of the ENJL model is to approximate large- N_c QCD at the chiral symmetry breaking scale Λ_χ by an effective four-fermion theory (generated by integration over quark and gluon fields above Λ_χ). The main assumption of this model is that higher dimension fermionic operators are irrelevant for long distances. The three parameters are the scale Λ_χ and the two coupling constants G_S and G_V of the four-fermion operators, respectively the scalar-pseudoscalar and the vector-axial ones. Alternatively one can trade these parameters for three other ones, i.e. the constituent quark mass, M_Q , the coupling of the constituent quarks to the pseudoscalar current, g_A , and the ratio M_Q^2/Λ_χ^2 .

Integration over quarks⁴ below Λ_χ (see [11] for the description of the method) yields the low-energy effective Lagrangians involving pseudoscalar mesons and the lowest spin-0 and spin-1 resonance. Within this context twenty-two low-energy constants have been derived in [11] and thirty-six others in [12]. Whenever there are experimental data, the ENJL prediction is in good agreement with them.

A calculation of the coupling constants d_1 and d_2 in the context of the chiral quark model which is nothing but the mean field approximation of the ENJL model, has been carried out in Ref. [4] (in this article however the operator modulated by d_3 in Eq. (11) has not been taken into account). In this mean field approximation one neglects the fluctuations of the resonances so that the calculation involves just one loop of a constituent quark of mass M_Q .

In the full ENJL model (see Ref. [11]) the quark-loop contribution is modified with respect to the mean-field approximation by the presence of the mixing axial-pseudoscalar parametrized by the constant g_A . In addition one gets contribution from integrating out the resonance fields. For any coupling our notation is (in what follows we shall drop the index ‘r’ of the coupling constants) $d_i = \tilde{d}_i + \sum_R d_i^R$ where \tilde{d}_i is the contribution of the quark loop and $\sum_R d_i^R$ stands for the sum of the contributions of the resonances ($R = S, V, A, T$).

Calculations have been performed with the Seeley-DeWitt expansion [21–23]⁵. For details of the procedure the reader can consult Ref. [11]. A brief summary is given in the appendix.

For all the numerical applications we shall use for the input parameters the values obtained in [11], Fit 1, i.e. $M_Q = 265$ MeV, $g_A = 0.61$ and $x = \frac{M_Q^2}{\Lambda_\chi^2} = 0.052$.

4.1. Quark-loop contribution

The results read

$$\tilde{d}_1 = -\frac{N_c}{16\pi^2} \frac{f_\pi^2}{M_Q^2} \frac{1}{24} \Gamma_2 g_A^2,$$

⁴ Here we disregard the gluonic fluctuations below Λ_χ (see [11] for a discussion of this issue).

⁵ In [4,13] an error in the coefficient H_4 of the expansion given in [23] has been pointed out. We use the correct expression for the coefficient which was already given in [22].

$$\begin{aligned}\tilde{d}_2 &= \frac{N_c}{16\pi^2} \frac{f_\pi^2}{M_Q^2} \frac{1}{48} \Gamma_2 g_A^2, \\ \tilde{d}_3 &= \frac{N_c}{16\pi^2} \frac{f_\pi^2}{M_Q^2} \frac{1}{48} \Gamma_1 \rho \quad \text{with} \quad \rho = \frac{M_Q f_\pi^2}{|\langle \bar{q}q \rangle|} = \frac{\Gamma_0}{\Gamma_{-1}} g_A,\end{aligned}\quad (23)$$

where we have used the shortened notation $\Gamma_n = \Gamma(n, M_Q^2/\Lambda_\chi^2)$ for the incomplete Gamma functions defined as follows:

$$\Gamma(n-2, x = M_Q^2/\Lambda_\chi^2) = \int_{M_Q^2/\Lambda_\chi^2}^{\infty} \frac{dz}{z} e^{-z} z^{n-2}. \quad (24)$$

For applications we use $\Gamma_1 = \Gamma_2 = 1$. When one sets $g_A = 1$ our results for $\tilde{d}_{1,2}$ coincide with those of the quark-loop calculation of [4] and do not agree with [13]. Concerning \tilde{d}_3 we disagree with the result extracted from Eq. (2.53) in the last paper of Ref. [13].

4.2. Spin-1 and spin-2 resonances

Here we shall follow the notations and definitions of [10–12]. The vector (respectively axial-vector) resonance field will be denoted by V_μ (respectively A_μ). We also define

$$R_{\mu\nu} = d_\mu R_\nu - d_\nu R_\mu, \quad \text{for} \quad R = V, A \quad \text{with} \quad d_\mu = \partial_\mu + \Gamma_\mu,$$

where Γ_μ is given by the expression

$$\Gamma_\mu = \frac{1}{2} \{ \xi^\dagger [\partial_\mu - i r_\mu] \xi - \xi [\partial_\mu - i l_\mu] \xi^\dagger \}. \quad (25)$$

Let us first consider the vector case. The coupling we are interested in is the one which modulates the operator $\epsilon^{\mu\nu\rho\sigma} \text{tr} (V_\mu \{ \xi_\nu, f_{\rho\sigma} \})$ called h_V . The $O(p^6)$ counterterms receive contributions from the exchange of ω^0 , ρ^0 and ϕ mesons. The last one will not be considered here since its contribution is suppressed by the large ϕ mass (the ϕ resonance contribution to the $\gamma\gamma \rightarrow \pi^0\pi^0$ amplitude has been included in Refs. [5,1]). Guided by the nonet assumption, we shall not use for the contribution of the ρ^0 meson the experimental data on the decay $\rho^0 \rightarrow \pi^0\gamma$ which have a large error, but instead those on the decay $\rho^+ \rightarrow \pi^+\gamma$. Then from $\Gamma(\rho^+ \rightarrow \pi^+\gamma)$ and $\Gamma(\omega^0 \rightarrow \pi\gamma)$ [8] one can extract

$$\frac{h_{\rho^+}}{M_{\rho^+}} \simeq 4.7 \cdot 10^{-5} \text{ MeV}^{-1} \quad \text{and} \quad \frac{h_{\omega^0}}{M_{\omega^0}} \simeq 4.9 \cdot 10^{-5} \text{ MeV}^{-1}, \quad (26)$$

and take, according to the nonet assumption, $\frac{h_{\rho^0}}{M_{\rho^0}} \equiv \frac{h_{\rho^+}}{M_{\rho^+}}$.

Within the ENJL model the constant h_V has been computed in [12]. Here we just recall the result

$$h_V = \frac{N_c}{16\pi^2} \frac{\sqrt{2}}{8f_V} (1 + g_A), \quad (27)$$

where f_V modulates the operator $\text{tr}(f_{\mu\nu}V^{\mu\nu})$ and has the following expression [11]

$$f_V^2 = \frac{N_c}{16\pi^2} \frac{2}{3} \Gamma_0. \quad (28)$$

Using the relation found in the ENJL model [11]

$$f_V M_V = \frac{f_\pi}{\sqrt{1 - g_A}}, \quad (29)$$

one obtains

$$\frac{h_V}{M_V} = \frac{N_c}{16\pi^2} \frac{\sqrt{2}}{8f_\pi} (1 + g_A) \sqrt{1 - g_A}. \quad (30)$$

Numerically one gets, for $g_A = 0.61$,

$$\frac{h_V}{M_V} = 3.6 \cdot 10^{-5} \text{ MeV}^{-1}. \quad (31)$$

For this constant the agreement of the ENJL prediction with experiment (26) is not as impressive as for the other low-energy constants. Moreover this quantity has to be squared in the contribution to the amplitude, so that finally the ENJL model prediction of d_i^V is a factor two smaller than the one based on resonance saturation. However one has to keep in mind that the coupling constants predicted in the ENJL model are parameters of the Green functions evaluated *at zero momenta*. This fact has to be taken into account, when comparing with processes, such as the decay of a vector resonance, whose typical energy scale is large. In [12] it was argued that including intermediate resonance exchanges and chiral loops one obtains an improved prediction in good agreement with the phenomenology of the vector resonance decay.

Whenever we deal with processes at small energy, such as Compton scattering at threshold for the determination of the pion polarizabilities, we favour the value of h_V predicted in the ENJL model. On the other hand, for the η decay the energy scale is quite close to the ρ mass and it seems appropriate to use for h_V the value extracted from experiments. Finally for the $\gamma\gamma \rightarrow \pi^0\pi^0$ transition we shall display two different cross-sections corresponding to the values of h_V obtained from ENJL and phenomenology, respectively. We take the difference between the cross-sections as a contribution to the uncertainty on our result.

The b_1 axial-vector resonance is not included in the ENJL model. We shall use the experimental data in order to incorporate it as it is done in [1].

The tensor resonance is not described either by the ENJL model. Such a resonance would appear only if higher derivative four-quark operators were taken into account. In this case again we shall use the experimental data. Unfortunately they allow only for a determination of the absolute value of the tensor contribution to the transitions considered here. Hence this contribution will appear as an uncertainty in our results.

4.3. Scalar resonance

The scalar-sector analysis requires the knowledge of the coupling constants C_S^d , C_S^m and C_S^γ which modulate respectively the operators $\text{tr}(S\xi_\mu\xi^\mu)$, $\text{tr}(S\chi^+)$ and $e^2 F_{\mu\nu}F^{\mu\nu} \times \text{tr}(SQ^2)$. The coupling constants C_S^d , C_S^m as well as the scalar mass M_S have been computed within the ENJL model in [11]. Their expressions reads

$$C_S^d = \frac{N_c}{16\pi^2} \frac{M_Q}{\lambda_S} 2g_A^2(\Gamma_0 - \Gamma_1), \quad (32)$$

$$C_S^m = \frac{N_c}{16\pi^2} \frac{M_Q}{\lambda_S} \rho(\Gamma_{-1} - 2\Gamma_0), \quad (33)$$

with the rescaling factor

$$\lambda_S^2 = \frac{N_c}{16\pi^2} \frac{2}{3}(3\Gamma_0 - 2\Gamma_1), \quad (34)$$

and the mass

$$M_S^2 = \frac{N_c}{16\pi^2} \frac{8M_Q^2}{\lambda_S^2} \Gamma_0. \quad (35)$$

Numerical evaluations for these constants can be found in [11] as well as the comparison with experiment and with the resonance saturation approach.

We have computed the coupling constant C_S^γ which governs the decay $S \rightarrow \gamma\gamma$ with the result

$$C_S^\gamma = \frac{N_c}{16\pi^2} \frac{2}{3} \frac{\Gamma_1}{M_Q \lambda_S}. \quad (36)$$

Numerically we find $C_S^\gamma \simeq 0.19 \text{ GeV}^{-1}$. This value is about a factor 2 larger than the estimate given in [1] (N.B. with an uncertainty of 100%). However it corresponds rather well to the estimate obtained in the analysis of [24], where higher order terms in the chiral expansion are taken into account, in order to match the QCD high energy behaviour.

The contributions of the scalar particle to the constants d_i (or $a_{1,2}$ and b) are given in [1] in terms of the mass M_S and the absolute values of the constants C_S^d , C_S^m , C_S^γ (in contrast with the resonance saturation calculation, here we know the sign of the different contributions). Within the ENJL model we find

$$d_1^S = 0, \quad (37)$$

$$d_2^S = \frac{C_S^\gamma C_S^d f_\pi^2}{8M_S^2} = \left(\frac{N_c}{16\pi^2} \frac{f_\pi^2}{M_Q^2} \right) \frac{1}{48} \frac{\Gamma_1}{\Gamma_0} g_A^2(\Gamma_0 - \Gamma_1), \quad (38)$$

$$d_3^S = \frac{C_S^\gamma C_S^m f_\pi^2}{8M_S^2} = \left(\frac{N_c}{16\pi^2} \frac{f_\pi^2}{M_Q^2} \right) \frac{1}{96} \frac{\Gamma_1}{\Gamma_0} \rho(\Gamma_{-1} - 2\Gamma_0). \quad (39)$$

We find $a_1^S \simeq 0.14$ and $a_2^S \simeq 4.7$ whereas the resonance saturation approach used in Ref. [1] gives $a_1^S \simeq \pm 0.8$ and $a_2^S \simeq \pm 1.3$.

A few comments are in order. First we have a definite prediction for the signs, even though it is very dependent on the input parameters in the case of a_1^S which is proportional to the difference of d_3^S and d_2^S , two quantities of comparable order of magnitude. Secondly and as a consequence of the latter remark we confirm the smallness of a_1^S . Finally we get for a_2^S (which is proportional to d_2^S) a sensibly higher value. This is related to the fact that in the ENJL model the constant C_S^γ computed in Eq. (36) appears to be higher than the estimate of [1] (but, as we said, this is in agreement with the recent analysis of [24]) and the scalar mass rather low (see [11,25]). At the present time it is not completely clear if the scalar contribution to the coupling constants predicted by the ENJL model is a better estimate than the analogous contribution calculated in [1]. Hence we keep the latter as a lower bound estimate and obtain in this way the uncertainty on the scalar contribution to the coupling constants.

In the next section we discuss a possible way of improving the situation in the future which is related to the coupling constant d_3 .

4.4. On the constant d_3

An interesting feature of the scalar sector is that within the ENJL model many cancellations occur between the quark-loop and the scalar resonance contributions. This is the case at $O(p^4)$ for the constants L_5 , L_8 and H_2 (see [11]). In our calculation, one finds that the combination $a_1^S + \tilde{a}_1$ is actually independent of the parameter ρ and of the quadratically divergent incomplete gamma function Γ_{-1} . For the full d_3 one obtains a quite simple expression

$$d_3 = d_3^S + \tilde{d}_3 = \left(\frac{N_c}{16\pi^2} \frac{f_\pi^2}{M_Q^2} \right) \frac{1}{96} g_A \Gamma_1. \quad (40)$$

Let us also notice that we get the following relation⁶:

$$\frac{C_S^\gamma}{C_S^d} = 8 \frac{d_3}{f_\pi^2 L_5}. \quad (41)$$

With the set of parameters we have already used one finds from Eq. (40) $d_3 \simeq 1.5 \times 10^{-5}$ whereas the value predicted in [1] using scalar resonance saturation is $d_3 \simeq 0.38 \times 10^{-5}$. The difference between these values comes both from d_3^S (which is already bigger in our case than the value of [1]) and from \tilde{d}_3 which is not present in the resonance saturation approach. One can compare both values with the estimate $d_3 = (0.94 \pm 0.47) \times 10^{-5}$ obtained in [26] using a sum rule for the vector-vector two-point function. This estimate is affected by a large uncertainty which makes it compatible with both our value and the value in [1] and so it does not provide a very satisfactory test.

An important improvement would be to extend this sum rule to two-loop order, as it is required by the fact that d_3 modulates an $O(p^6)$ operator. Hence it is a bit premature to try to improve the agreement of our result with the sum-rule, which could be achieved

⁶ Which is valid to all orders in the $\alpha_S N_c$ -expansion (see Ref. [11]).

Table 1
Final results

	Q.L.	(1 ⁻⁻)		(1 ⁺⁻)	(0 ⁺⁺)		(2 ⁺⁺)	Total
		ENJL	Data		ENJL	Data		
a_1	-12.3	-20.3	-36.6	0	0.14	0.8	∓ 4.1	$-28 \geq a_1 \geq -53$
a_2	6.1	7.6	13.7	-1.3	4.7	1.3	± 1.0	$13 \leq a_2 \leq 24$
b	1.0	1.3	2.3	0.7	0	0	± 0.5	$2 \leq b \leq 4$

by changing slightly the value of the parameters M_Q and g_A and redoing the fits of Ref. [11] including d_3 ; this would of course have an effect on all the $O(p^6)$ constants. We postpone such considerations until a full two-loop calculation of the sum-rule is carried out.

5. Results

5.1. $\gamma\gamma \rightarrow \pi^0\pi^0$

In the Table we display the full ENJL results for the constants a_1 , a_2 and b to be compared with Table 2 in [1].

Inspection of the Table shows that we have three sources of uncertainties. The first two are related to the different estimates of the vector and scalar coupling constants obtained in Section 4 by using ENJL and experimental data, respectively⁷. In the last column we have added these uncertainties in such a way as to have an upper bound and a lower bound for the cross-section. This is because the uncertainties on the vector (see Section 4.2) and the scalar resonance (see Section 4.3) contribution have different origins. The last uncertainty comes from the sign of the tensor contribution which is undetermined. We included also this contribution in the total (last column of the Table).

For the low-energy constants entering the helicity amplitudes we get

$$\begin{aligned}
 -8 &\geq h_+ = a_1 + 8b \geq -17, \\
 8 &\leq h_s = a_2 - 2b \leq 15, \\
 2 &\leq h_- = b \leq 4.
 \end{aligned}
 \tag{42}$$

Our results are compatible with those quoted in [1]:

⁷We assume the central value of the experimental data, ignoring the errors on the measured parameters (which typically have a 10% size). In addition, we disregard the changes in the ENJL prediction due to variations of the three parameters of the model. In our opinion, assuming the quite large band of error on the cross-section associated to the ENJL prediction and the experimental estimate for the resonance contributions, is pessimistic enough.

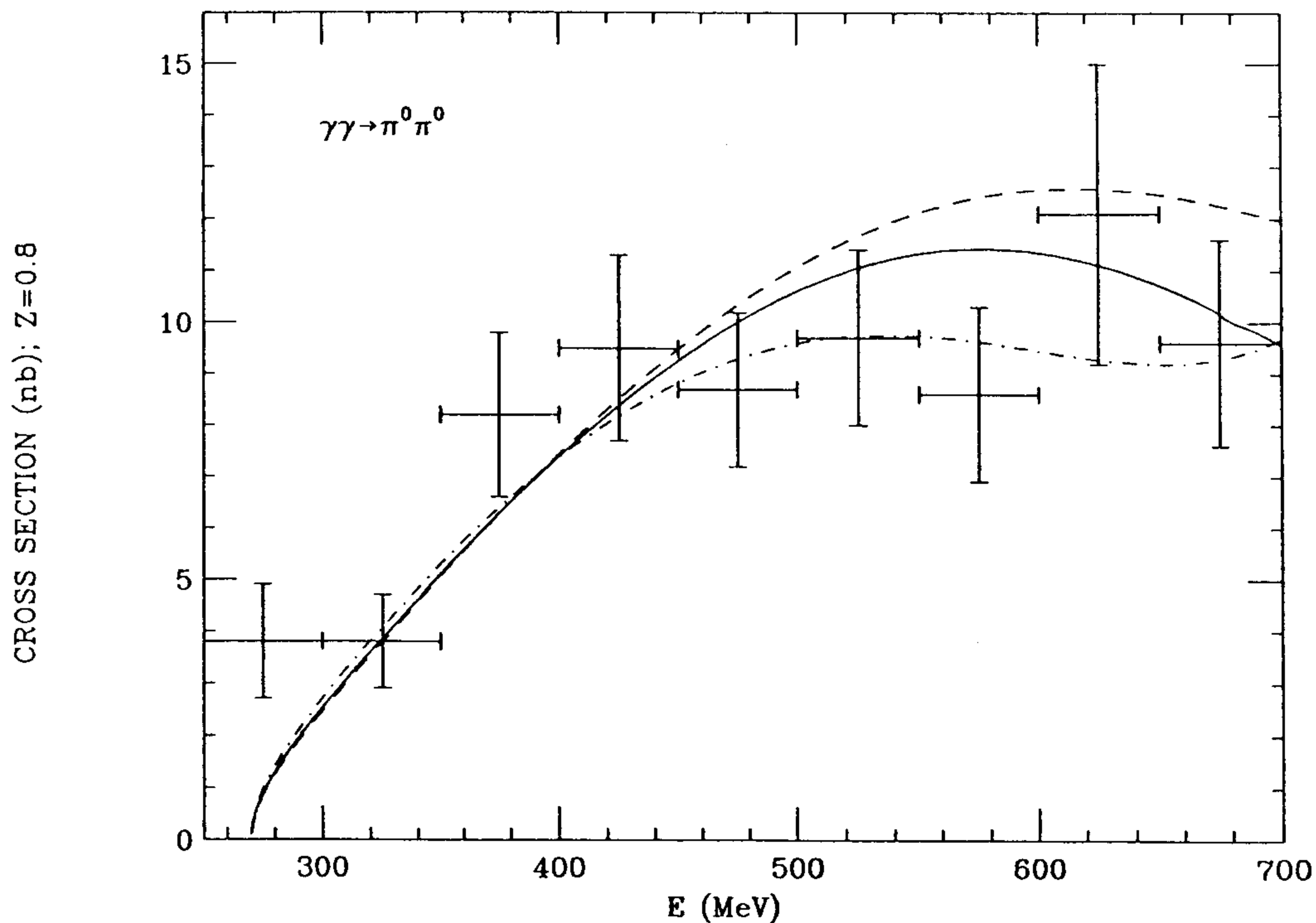


Fig. 1. The $\gamma\gamma \rightarrow \pi^0\pi^0$ cross section $\sigma(s; |\cos\theta| \leq Z)$ as a function of the center-of-mass energy E at $Z = 0.8$, and the data from Crystal Ball [2]. The solid and dash-dotted lines are the $O(p^6)$ results obtained from the ENJL model. They correspond to the values in the l.h.s. and, respectively, the r.h.s of the inequalities (42). The dashed line is the two-loop result obtained with resonance saturation in [1]. It coincides with the solid lines in Figs. 5, 11 of [1].

$$\begin{aligned}
 h_+ &= -14 \pm 5, \\
 h_s &= 7 \pm 3, \\
 h_- &= 3 \pm 1.
 \end{aligned}
 \tag{43}$$

In the Figure we display the data from Ref. [2] for the cross-section $\sigma(s; |\cos\theta| \leq Z = 0.8)$ as a function of the center-of-mass (c.m.) energy $E = \sqrt{s}$. The solid (respectively, dash-dotted) line in the Figure corresponds to the values in the l.h.s. (respectively, the r.h.s.) of the inequalities (42). For comparison we show in the Figure, as a dashed line, also the cross-section obtained in [1] for the central values of (43) (see the solid lines in Figs. 5, 11 of Ref. [1]). We can also compare our results with Fig. 9 of Ref. [1], where the uncertainties in the values of (43) are taken into account (in Fig. 9 of Ref. [1], however, the contribution of the integrals $\Delta_{A,B}$ coming from the two-loop box and the acnode diagrams in Fig. 4 and appearing in Eqs. (7.3), (7.8) of [1] is neglected, whereas in our Figure the full contribution is retained). This comparison shows that our results are compatible with those of [1]. The upper curve in Fig. 9 of Ref. [1] disagrees with our result by more than 20% for c.m. energies $E \geq 540$ MeV (at $E = 540$ MeV the $\Delta_{A,B}$ contribution to the cross-section is very small, i.e. 1.5%, see Figs. 5, 9 of [1]).

5.2. $\eta \rightarrow \pi^0 \gamma \gamma$

As we said in Section 3.2 the $O(p^6)$ counterterms contribution is expected to account for a large part of the amplitude because the loop contributions are suppressed. In Ref. [7] it is shown that the resonance saturation approximation is not sufficient to explain the experimental decay rate. Indeed if one takes into account only vector resonance saturation one gets

$$\Gamma(\eta \rightarrow \pi^0 \gamma \gamma) \simeq 0.18 \text{ eV}, \quad (44)$$

to be compared with the experimental value [8] $\Gamma(\eta \rightarrow \pi^0 \gamma \gamma) \simeq 0.85 \pm 0.18 \text{ eV}$. Let us review the calculation of [7]. By keeping the momenta dependence in the vector propagator the authors of [7] made an ‘all-order’ estimate, i.e. at $O(p^6)$ and higher, of the counterterms contribution with the result

$$\Gamma(\eta \rightarrow \pi^0 \gamma \gamma) \simeq 0.31 \text{ eV}. \quad (45)$$

Then if in addition one takes into account chiral loops (the $O(p^4)$ ones as well as the $O(p^8)$ ‘doubly-anomalous’ one-loop diagrams) one reaches the value

$$\Gamma(\eta \rightarrow \pi^0 \gamma \gamma) = 0.42 \pm 0.20 \text{ eV}, \quad (46)$$

where the error includes scalar and tensor contributions (whose sign was not known) as well as a 30% error coming from other contributions such as one-loop diagrams involving the $O(p^6)$ Lagrangian (11).

Let us now show step by step the ENJL results. To the estimate (44) which incorporates only vector resonance exchange, we first add quark loop contribution and find

$$\Gamma(\eta \rightarrow \pi^0 \gamma \gamma) \simeq 0.36 \text{ eV}. \quad (47)$$

Already we are not far from the central value of Eq. (46). In addition if we include the scalar contribution as predicted by ENJL we have

$$\Gamma(\eta \rightarrow \pi^0 \gamma \gamma) \simeq 0.5 \text{ eV}. \quad (48)$$

We shall use as lower bound the prediction for the scalar exchange given in [1]. Then we have

$$\Gamma(\eta \rightarrow \pi^0 \gamma \gamma) = 0.45 \pm 0.05 \text{ eV}. \quad (49)$$

Finally taking into account the axial resonance and, as in [7], the contributions from chiral loops and, in addition, an uncertainty from the contribution of the tensor resonance, we get

$$\Gamma(\eta \rightarrow \pi^0 \gamma \gamma) = 0.58 \pm 0.12 \text{ eV}. \quad (50)$$

Of course we can play the game of making an ‘all-order’ estimate of the counterterm given by vector resonance exchange as it is done in [7]. Starting from the upper

bound in the last equation, we obtain a decay rate of 0.86 eV. However this represents only a partial resummation of the chiral corrections. First there are $O(p^8)$ one-loop corrections involving the $O(p^6)$ Lagrangian (11) which could be as important as the counterterms contributions (even though they are next-to-leading in $1/N_c$). Secondly, in the large N_c -limit, other chiral corrections (i.e. of $O(p^8)$ and higher) coming from the counterterms occur within the ENJL model. Indeed the quark-loop contribution considered here corresponds to the computation of a four-point function at zero momenta. The full ENJL calculation at non-zero momenta (as it has been done in [27] for the two-point and some of the three-point functions) would bring additional chiral corrections. We shall include all chiral corrections of this type in an additional 30% uncertainty. Our prediction is then

$$\Gamma(\eta \rightarrow \pi^0 \gamma \gamma) = 0.58 \pm 0.3 \text{ eV}. \quad (51)$$

As we said above, the higher order corrections included in the ‘all-order’ estimate of the vector resonance contribution enhance the decay width and therefore go in the right direction, in order to match the experimental result $\Gamma(\eta \rightarrow \pi^0 \gamma \gamma) = 0.85 \pm 0.18 \text{ eV}$. It would be interesting to carry out the $O(p^8)$ loop analysis (this can be done, given that most of the loop diagrams are suppressed (see Section 3.2)), as well as to calculate in the ENJL model the $O(p^8)$ counterterms. In this way one could obtain an accurate description of the $O(p^8)$ chiral corrections.

5.3. Polarizabilities

The pion polarizabilities have been estimated through dispersion sum rules [18]

$$\begin{aligned} (\alpha - \beta)^N &= -10 \pm 4, \\ (\alpha + \beta)^N &= 1.04 \pm 0.07. \end{aligned} \quad (52)$$

At order $O(p^6)$ resonance saturation gives [1]

$$\begin{aligned} (\alpha - \beta)^N &= -1.01 - 0.31 - 0.58 \pm 0.20 = -1.90 \pm 0.20, \\ (\alpha + \beta)^N &= 0.00 + 0.17 + 1.00 \pm 0.30 = 1.17 \pm 0.30, \end{aligned} \quad (53)$$

where the three contributions that add up to the final results on the r.h.s. are the one-loop result, the two-loop contribution, and the one from the $O(p^6)$ counterterms assuming resonance saturation, respectively. There is a large contribution from the $O(p^6)$ low-energy constants due mainly to the ω -exchange in the resonance saturation approach [28]. For the estimate of the uncertainties in (53) the reader is invited to consult Ref. [1].

The contribution due to the $O(p^6)$ counterterms to the pion polarizabilities

$$\begin{aligned} (\alpha - \beta)_{\text{c.t.}}^N &= \frac{\alpha m_\pi}{(4\pi f_\pi)^4} h_+, \\ (\alpha + \beta)_{\text{c.t.}}^N &= \frac{\alpha m_\pi}{(4\pi f_\pi)^4} 8h_-, \end{aligned} \quad (54)$$

is obtained from the ENJL model prediction for the low-energy constants displayed in Eqs. (42)

$$\begin{aligned} -0.33 &\geq (\alpha - \beta)_{\text{c.t.}}^N \geq -0.69, \\ 0.78 &\leq (\alpha + \beta)_{\text{c.t.}}^N \leq 1.44. \end{aligned} \quad (55)$$

Adding the one-loop and two-loop contributions – identical to those in (53) – we get our results with the ENJL model

$$\begin{aligned} -1.65 &\geq (\alpha - \beta)^N \geq -2.01, \\ 0.95 &\leq (\alpha + \beta)^N \leq 1.61, \end{aligned} \quad (56)$$

which are compatible with Eqs. (53). Both the prediction in (56) and the result in [1] are compatible with the forward sum rule $(\alpha + \beta)^N = 1.04 \pm 0.07$ in (52).

As we mentioned in Section 4.2, we consider the ENJL value of the vector resonance coupling as favoured. This choice corresponds to the range of values $-1.65 \geq (\alpha - \beta)^N \geq -1.68$ and $0.95 \leq (\alpha + \beta)^N \leq 1.28$. Here the residual uncertainty for $(\alpha - \beta)^N$ reflects an incomplete knowledge (see Section 4.3) in estimating the coupling constants for the scalar resonance, whereas the undetermined sign of the tensor contribution to the low-energy constants in the Table yields the remaining uncertainty on $(\alpha + \beta)^N$. The sizeable difference between the value of $(\alpha - \beta)^N$ obtained using the ENJL prediction for the vector resonance coupling and the result (53) is mainly due to the fact that the ENJL prediction of the vector contribution to h_+ is a factor two smaller than the one based on resonance saturation and the experimental data (see Section 4.2). The size of the quark-loop contribution, which is included in the ENJL prediction, is not large enough, to bring the ENJL value for h_+ to the one obtained from resonance saturation.

The construction of unitarized S -wave amplitudes for $\gamma\gamma \rightarrow \pi\pi$ which contain $(\alpha - \beta)^{C,N}$ as adjustable parameters has been carried out in Ref. [29]. In this case, only $(\alpha - \beta)^{C,N}$ can be determined from the data [2,30], with the result [29]

$$\begin{aligned} (\alpha - \beta)^C &= 4.8 \pm 1.0, \\ (\alpha - \beta)^N &= -1.1 \pm 1.7. \end{aligned} \quad (57)$$

The value (57) for $(\alpha - \beta)^N$ is consistent with the two-loop result for the neutral pion, both for the calculation based on resonance saturation [1] and for the ENJL prediction, whereas the corresponding two-loop calculation for charged pions is not available and so it cannot be compared with the value (57) for $(\alpha - \beta)^C$.

In [31] the validity of the errors quoted in a recent estimate of $(\alpha + \beta)^{C,N}$ by Kaloshin and collaborators [32] is questioned. Here the polarizabilities appear as adjustable parameters in the unitarized D -wave amplitudes, hence the values of $(\alpha + \beta)^{C,N}$ can be determined from the data with the result [32]

$$\begin{aligned} (\alpha + \beta)^C &= 0.22 \pm 0.06 & [30], \\ (\alpha + \beta)^N &= 1.00 \pm 0.05 & [2]. \end{aligned} \quad (58)$$

The authors of [31], arguing on the partial wave analysis of the data that shows large uncertainties even at the $f_2(1270)$ mass, conclude that the errors quoted in (58) for $(\alpha + \beta)^N$ are unbelievably small. This result is compatible with the ENJL prediction (56), as well as with the value in (53).

6. Conclusion

Within the ENJL model we have computed the $O(p^6)$ coupling constants entering the χ PT expansion for the amplitudes of $\gamma\gamma \rightarrow \pi^0\pi^0$ and $\eta \rightarrow \pi^0\gamma\gamma$. In addition to the contribution of the resonance exchange, one has to add terms coming from the constituent quark loop. Both contributions have comparable orders of magnitude. This situation at $O(p^6)$ differs from the one at $O(p^4)$, which is described in [11].

Our major result concerns the decay $\eta \rightarrow \pi^0\gamma\gamma$, where the contribution of the counterterms dominates the amplitude. The values of the couplings calculated in the ENJL model yield a prediction for the decay width which is compatible with the data. Our central value compares much more favourably with the experimental result [8] than the value calculated in [7] within resonance saturation.

Concerning the transition $\gamma\gamma \rightarrow \pi^0\pi^0$, our results are compatible with those of the resonance saturation approach worked out by [1], as well as with the data [2]. For the neutral pion polarizabilities, we find results consistent with the estimates given in earlier references [1,29,32].

To improve our knowledge of the coupling constants d_i 's and be able to test in a more accurate way the ENJL prediction, we need both experimental and theoretical progress.

High-precision data from DAΦNE on $\gamma\gamma \rightarrow \pi^0\pi^0$ may allow to extract the value of h_s , since the cross-section in Fig. 9 of [1] shows a sizeable dependence on this low-energy constant for energies near 600 MeV. It will be necessary to carry out a unitarization of the two-loop result, using a procedure analogous to [33] and matching the dispersive calculation for the all-order amplitude with the two-loop amplitudes for $\gamma\gamma \rightarrow \pi^0\pi^0$ and $\gamma\gamma \rightarrow \pi^+\pi^-$, once the latter will have been calculated. The consideration of this improved, unitarized amplitude will justify the inclusion in the analysis of experimental data up to 600 MeV.

For the other source of information, i.e. the decay $\eta \rightarrow \pi^0\gamma\gamma$, it will be very interesting to investigate the $O(p^8)$ analysis, as we said in Section 5.2. The crucial test may be the future SATURNE experiments which may allow to determine d_1 , d_2 as well as the size of the $O(p^8)$ chiral corrections.

Finally the determination of the constant d_3 from the sum-rule has to be improved by carrying out the computation to the two-loop order.

Acknowledgements

We are pleased to thank Ll. Ametller, J. Bijnens, A. Bramon, J. Gasser, J. Prades, E. de Rafael, M.E. Sainio and J. Stern for useful discussions. We wish to thank A. Schaale, S. Scherer and the referee of the paper for calling Ref. [13] to our attention.

Appendix

Let us define

$$\begin{aligned}\nabla_\mu &= \partial_\mu + \mathcal{A}_\mu, \\ \mathcal{A}_\mu &= \Gamma_\mu - \frac{i}{2} \gamma_5 (g_A \xi_\mu + W_\mu^{(-)}) - \frac{i}{2} W_\mu^{(+)}. \end{aligned}$$

Let us also introduce the following expression:

$$M = -M_Q - S - \frac{1}{2} (\Sigma - \gamma_5 \Delta),$$

where

$$\begin{aligned}\Sigma &= \xi^\dagger \mathcal{M} \xi^\dagger + \xi \mathcal{M}^\dagger \xi, \\ \Delta &= \xi^\dagger \mathcal{M} \xi^\dagger - \xi \mathcal{M}^\dagger \xi. \end{aligned}$$

Here S , $W_\mu^{(+)}$ and $W_\mu^{(-)}$ denote the fields of the resonances, respectively scalar, vector and axial-vector.

We recall briefly the Seeley-DeWitt expansion of the operator

$$\mathcal{D}_E^\dagger \mathcal{D}_E - M_Q^2 = -\nabla_\mu \nabla_\mu + E,$$

where \mathcal{D}_E is the Euclidean Dirac operator

$$\mathcal{D}_E = \gamma_\mu \nabla_\mu + M,$$

and

$$E = 2M_Q S + iM_Q \gamma_\mu \gamma_5 g_A \xi_\mu - \frac{1}{4} \sigma_{\mu\nu} f_{\mu\nu} + \dots$$

(here we do not need the complete expression which can be found in [11]).

The effective action reads then

$$\Gamma_E = -\frac{1}{2} \int_{1/\Lambda_x^2}^{\infty} \frac{d\tau}{\tau} \text{Tr} \exp(-\tau \mathcal{D}_E^\dagger \mathcal{D}_E) = -\frac{1}{2} \frac{N_c}{16\pi^2} \sum_{n=0}^{\infty} \frac{\Gamma(n-2, x)}{(M_Q^2)^{n-2}} \text{tr} H_n,$$

in terms of the incomplete Gamma functions defined in (24). We give the Seeley-DeWitt coefficients up to a total derivative and a circular permutation. Only the terms we are interested in are displayed here. These terms read

$$\begin{aligned}
 H_3 &= -\frac{1}{6} \left\{ E^3 + \frac{1}{2} ER_{\mu\nu}R_{\mu\nu} \right\}, \\
 H_4 &= \frac{1}{24} \left\{ E^4 + \frac{1}{5} [ER_{\mu\nu}ER_{\mu\nu} + 4E^2R_{\mu\nu}R_{\mu\nu}] \right\}.
 \end{aligned}
 \tag{59}$$

Note added

A calculation of the $O(p^6)$ Lagrangian within the ENJL model, but without including the contribution of resonance exchange, can be found in [13]. Notice that a complicated expression for the Seeley-DeWitt coefficients displayed in [13] reduces to the very simple expression (59) in our appendix, owing to the presence of just neutral external particles in the reactions considered in the present work. However, the calculations of [13] do not reproduce the results obtained in the mean field approximation by the authors of Ref. [4] using two different approaches, i.e. both by means of the coefficients of heat kernel expansion and by directly calculating the Feynman diagrams. Our calculation reproduces the mean field results of [4].

References

- [1] S. Bellucci, J. Gasser and M.E. Sainio, Nucl. Phys. B 423 (1994) 80; B 431 (1994) 413 (E).
- [2] The Crystal Ball Collaboration, H. Marsiske et al., Phys. Rev. D 41 (1990) 3324.
- [3] P. Ko, Phys. Rev. D 41 (1990) 1531.
- [4] J. Bijnens, S. Dawson and G. Valencia, Phys. Rev. D 44 (1991) 3555.
- [5] S. Bellucci and D. Babusci, in: Proceedings of the Workshop on Physics and Detectors for DAΦNE, Frascati, 1991, ed. G. Pancheri (INFN, Frascati, 1991) p. 351.
- [6] S. Bellucci, in: The DAΦNE Physics Handbook, eds. L. Maiani, G. Pancheri and N. Paver (INFN, Frascati, 1992) p. 419.
- [7] Ll. Ametller, J. Bijnens, A. Bramon and F. Cornet, Phys. Lett. B 276 (1992) 185.
- [8] Particle Data Group, M. Aguilar-Benitez et al., Phys. Rev. D 50 (1994) 1173.
- [9] G. Ecker, J. Gasser, A. Pich and E. de Rafael, Nucl. Phys. B 321 (1989) 311; J.F. Donoghue, C. Ramirez and G. Valencia, Phys. Rev. D 39 (1989) 1947; M. Praszalowicz and G. Valencia, Nucl. Phys. B 341 (1990) 27.
- [10] G. Ecker, J. Gasser, H. Leutwyler, A. Pich and E. de Rafael, Phys. Lett. B 223 (1989) 425.
- [11] J. Bijnens, C. Bruno and E. de Rafael, Nucl. Phys. B 390 (1993) 501.
- [12] J. Prades, Z. Phys. C 63 (1994) 491.
- [13] D. Ebert, A.A. Belkov, A.V. Lanyov and A. Schaale, Int. J. Mod. Phys. A 8 (1993) 1313; A.A. Belkov, A.V. Lanyov and A. Schaale, Radiative Kaon Decays and CP Violation, hep-ph/9305330; A.A. Belkov, A.V. Lanyov, A. Schaale and S. Scherer, preprint TRI-PP-94-69.
- [14] J. Gasser and H. Leutwyler, Nucl. Phys. B 250 (1985) 465.
- [15] J. Bijnens and F. Cornet, Nucl. Phys. B 296 (1988) 557.
- [16] J.F. Donoghue, B.R. Holstein and Y.C. Lin, Phys. Rev. D 37 (1988) 2423.
- [17] J.F. Donoghue, B.R. Holstein and Y.-C.R. Lin, Phys. Rev. Lett. 55 (1985) 2766; J. Bijnens, A. Bramon and F. Cornet, Phys. Rev. Lett. 61 (1988) 1453.
- [18] For reviews on polarizabilities see e.g., V.A. Petrunkin, Sov. J. Part. Nucl. 12 (1981) 278; J.L. Friar, in: Proc. of the Workshop on Electron-Nucleus Scattering, Marciana Marina, 7-15 June 1988, eds. A. Fabrocini et al. (World Scientific, Singapore, 1989) p. 3; B.R. Holstein, Comments Nucl. Part. Phys. 19 (1990) 221; M.A. Moinester, in: Proc. 4th Conf. on the Intersections Between Particle and Nuclear Physics, Tucson, Arizona, May 24-29, 1991, AIP Conf. Proc. No. 243, ed. W.T.H. Van Oers (AIP, New York, 1992) p. 553.

- [19] J.F. Donoghue and B.R. Holstein, *Phys. Rev. D* 40 (1989) 2378.
- [20] D. Babusci et al., in: *Proceedings of the Workshop on Physics and Detectors for DAΦNE, Frascati, 1991*, ed. G. Pancheri (INFN, Frascati, 1991) p. 383;
D. Babusci et al., *Phys. Lett. B* 277 (1992) 158.
- [21] B. DeWitt, *Dynamical Theory of Groups and Fields* (Gordon and Breach, New York, 1965);
R. Seeley, *Am. Math. Soc. Proc. Symp. Pure Math.* 10 (1967) 288.
- [22] A.E.M. van de Ven, *Nucl. Phys. B* 250 (1985) 593.
- [23] R.D. Ball, *Phys. Rep.* 182 (1989) 1.
- [24] B. Moussallam and J. Stern, Orsay Preprint IPNO/TH 94-26.
- [25] J. Bijnens, E. de Rafael and H. Zheng, *Z. Phys. C* 62 (1994) 437.
- [26] M. Knecht, B. Moussallam and J. Stern, Orsay Preprint IPNO/TH 94-08.
- [27] J. Bijnens and J. Prades, *Z. Phys. C* 64 (1994) 475.
- [28] D. Babusci, S. Bellucci, G. Giordano and G. Matone, *Phys. Lett. B* 314 (1993) 112.
- [29] A.E. Kaloshin and V.V. Serebryakov, Irkutsk preprint ISU-IAP.Th93-03 (hep-ph/9306224).
- [30] The Mark II Collaboration, J. Boyer et al., *Phys. Rev. D* 42 (1990) 1350.
- [31] J. Portolés and M.R. Pennington, in: *The Second DAΦNE Physics Handbook*, eds. L. Maiani, G. Pancheri and N. Paver (INFN, Frascati, 1994).
- [32] A.E. Kaloshin, V.M. Persikov and V.V. Serebryakov, Irkutsk preprint ISU-IAP.Th94-01.
- [33] J.F. Donoghue and B.R. Holstein, *Phys. Rev. D* 48 (1993) 137.